Quasi-three dimensional hydraulic design and performance calculation of high specific speed mixed-flow pump

M Su[1], Y X Zhang[2], J Y Zhang[2] and H C Hou[2]

1. China Petroleum Engineering Co., Ltd., Beijing Company, Beijing 100085, China
2. College of Mechanical and Transportation Engineering, China University of Petroleum, Beijing,102249, China

E-mail: jqsumin@163.com

Abstract. According to the basic parameters of 211-80 high specific speed mixed-flow pump, based on the quasi-three dimensional flow theory, the hydraulic design of impeller and its matching spaced guide vanes for high specific speed mixed flow pump was completed, in which the iterative calculation of S_1, S_2 stream surfaces was employed to obtain meridional flow fields and the point-by-point integration method was employed to draw blade camber lines. Blades are thickened as well as blade leading edges are smoothed in the conformal mapping surface. Subsequently the internal fields of the whole flow passage of the designed pump were simulated by using RANS equations with RNG $k-\varepsilon$ two-equation turbulent model. The results show that, compared with the 211-80 model, the hydraulic efficiency of the designed pump at the optimal flow rate increases 9.1%. The hydraulic efficiency of designed pump in low flow rate condition (78% designed flow rate) increases 6.46%. The hydraulic efficiency in high flow rate areas increases obviously and there is no bad phenomenon of suddenly decrease of hydraulic efficiency in model pump. From the distributions of velocity and pressure fields, it can be seen that the flow in impeller is uniform and the increase of pressure is gentle. There are no obvious impact phenomenon on impeller inlet and obvious wake shedding vortex phenomenon from impeller outlet to guide vanes inlet.

1. Introduction

With more attention of national economic development is paid on energy conservation and emission reduction, the high specific speed mixed-flow pumps with high hydraulic efficiency, strong cavitation erosion resistance, excellent running stability are required urgently. At the present stage, the pump design usually adopts similar conservation method or speed coefficient method based on the similarity theory, or hydraulic design method based on one dimensional or two dimensional theories, but these methods are empirical and design qualities largely depend on experience of designers and improvement after hydraulic performance tests [1]. It is not common for hydraulic design by using quasi-three dimensional or three dimensional methods. Based on the two families of stream surfaces theory, Binghao et al. put forward the direct and inverse problem iterative design method of mixed-flow pump impeller and complete the design of impeller of mixed-flow pump which specific speed is 348[2]. This method can effectively make up for the defect of traditional design method which the calculation of meridional flow only satisfies the fluid continuous equation. Otherwise, the influence of blade shape on the calculation of meridional flow field is also considered. However, there are relatively less researches on high specific speed mixed-flow pump based on quasi-three dimensional

theory. On one hand, for the restriction of specific speed, the specific speed is generally from 200 to 500 in the traditional hydraulic design of mixed-flow pump model impellers. With the increase of specific speed, axial flow pumps are for most use and there are not good similar model pumps for reference. In addition, the development of high specific mixed-flow pumps becomes more and more difficult with the uncertainty of empirical parameters selection based on quasi-three dimensional hydraulic design method. On the other hand, due to the complex structure of high specific speed mixed-flow pump, there are obvious bend torsion characteristics of impeller blades. Otherwise, the shape of hub, the clearance between impeller and shroud as well as the clearance between impeller and guide vanes have obvious influences on the three-dimensional unsteady turbulent flow of high specific mixed-flow pump. Up to now, the cognition that people on the inner flow of high specific mixed-flow pump is limited [3, 4].

According to the basic parameters of 211-80 high specific speed mixed-flow pump [5], based on the quasi-three dimensional theory, the self-complied program is adopted to complete the hydraulic design of new mixed-flow pump. The internal flow fields of the designed pump were simulated by using RANS equations with RNG $k-\varepsilon$ two-equation turbulent model. The purpose of this paper is to explore a new rapid development method of high specific mixed-flow pumps.

2. Quasi-three dimensional hydraulic design

The quasi-three dimensional hydraulic design of designed pump is completed by calculation procedure (Program flow chart is shown in figure 1).

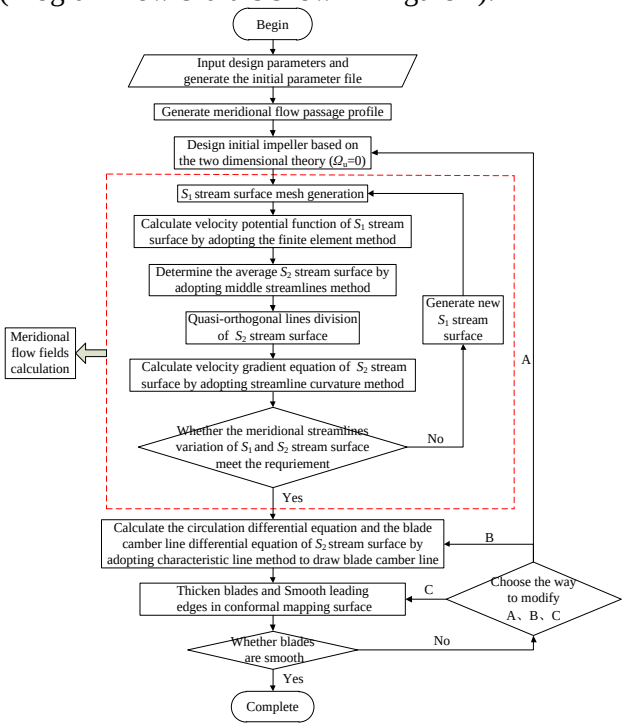

The concrete steps are:

① The initial axial flow passage profile is completed based on the basic design parameters ($Q_d = 1440$ m^3/h, $H = 6.53$ m, $n = 1450$ r/min).

②The initial impeller and spaced guide vanes designed based on the two dimensional theory ($\Omega_u = 0$).

③ The iterative calculation of S_1 stream surface and S_2 stream surface is conducted.

④ The point-by-point integrate method is applied to draw blade camber line according to the meridional velocity distribution obtained from step ③.

⑤ Blade thickening and smoothing are completed in conformal mapping surface.

Figure 1. The flow chart of quasi-three dimensional hydraulic design

2.1. Initial impeller confirmation

The specific speed of designed mixed-flow pump is $n_s = \dfrac{3.65n\sqrt{Q}}{H^{3/4}} = 819$. According to the basic parameters of 211-80 high specific speed mixed-flow pump, combined with traditional speed coefficient method, the initial impeller flow passage profile is determined by referring to the similar specific speed hydraulic model. In order to adapt to the operating condition regulation, the adjustable blade design method is adopted to guarantee the high efficient operating in a wide range of flow rate

and head. The blade area is designed as hemispherical and the inlet and outlet of blade are smoothed by arc. The angle between the blade rotational axis and pump axis is normally chosen as $\theta_d = 45° \sim 60°$ and the high specific speed pumps chose the great value. The designed pump chooses as 55 °. The range of hub ratio is 0.45~0.65. The designed pump chooses as 0.52. Figure 2 is the profile of meridional flow passage of impeller. The initial impeller is confirmed after the determination of the profile of meridional flow passage based on two dimensional flow theory ($\Omega_u = 0$) [6].

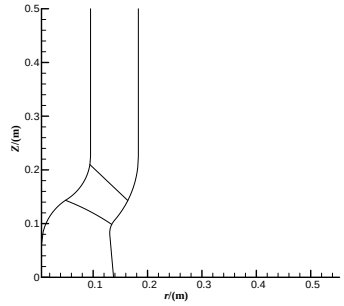

Figure 2. Impeller meridional flow passage profile

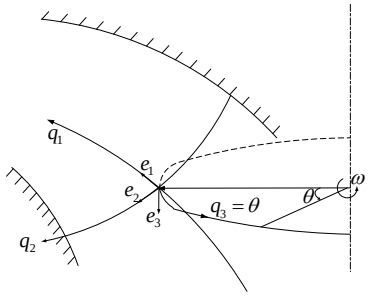

Figure 3. Orthogonal curvilinear coordinate

2.2. Meridional flow field calculation

The calculation of meridional flow field is to use the geometry and flow boundary conditions of whole flow domain formed by the flow passage of initial impeller and guide vanes to achieve. The orthogonal curvilinear is adopted for calculation (shown in figure 3), q_1, q_2 and q_3 represent the direction of meridional streamlines, water section lines and peripheral direction respectively. The basic suppose of steady, incompressible, non-viscous, irrotational and only gravity is introduced. The flow of S_1 stream surface is supposed irrational and the flow of S_2 stream surface is axial symmetry. Where, $H_1 = H_1(q_1, q_2)$, $H_2 = H_2(q_1, q_2)$, $H_3 = r$, $\upsilon_1 = w_1$, $\upsilon_2 = w_2$, $\upsilon_3 = w_3 + r\omega$.

Supposing the absolute motion of the coming flow of impeller is irrational ($\nabla \times \boldsymbol{v} = 0$). There is the corresponding three dimensional potential function ($\nabla \times \boldsymbol{v} = 0$). So, the calculation of the flow of S_1 stream surface transfers to the calculation of velocity potential function φ. The conformal transformation [7] is introduced, so the potential function equation of S_1 stream surface on conformal surface (x-y surface) can be expressed by the follow equation,

$$\begin{cases} \dfrac{\partial}{\partial x}\left(h\dfrac{\partial \varphi}{\partial x}\right) + \dfrac{\partial}{\partial y}\left(h\dfrac{\partial \varphi}{\partial y}\right) = 0 \\ h = h(y) \end{cases} \tag{1}$$

Where, h represents the flow layer thickness of S_1 stream surface.

Ritz variation is introduced to solve potential function (1) by giving the inlet, outlet, surface and periodic boundary conditions. The variation function is as follow，

$$I = -\frac{1}{2}\iint_D h\left[\left(\frac{\partial \varphi}{\partial x}\right)^2 + \left(\frac{\partial \varphi}{\partial y}\right)^2\right]\mathrm{d}x\mathrm{d}y + \oint_{\partial\Omega} h\frac{\partial \varphi}{\partial n}\varphi \mathrm{d}S$$

The finite element method is adopted for numerical solution.

For average S_2 stream surface ($q_2 = const$), q_1 is independent variable which represents coordinate surface of streamlines. So there is $\upsilon_2 = w_2 = 0$ (υ_i represents the absolute velocity component, w_i is velocity component of relative coordinate). The flow passage of impeller and spaced guide vans is divided into blade section and non-blade section. The corresponding meridional velocity gradient equation is,

a) The velocity gradient equation in blade section is,

$$\frac{\mathrm{d}\upsilon_1}{\mathrm{d}l} = A\upsilon_1 + B + \frac{C}{\upsilon_1} \tag{2}$$

where,

$$A = \frac{1}{1+\left(r\frac{\partial\theta}{\partial m}\right)^2}\left[-\left(\frac{1}{\tau}\frac{\partial\tau}{\partial m}+\frac{\sin\gamma}{r}+\frac{1}{\cos\delta}\frac{d\gamma}{dl}\right)\left(\sin\delta + r^2\frac{d\theta}{dl}\frac{\partial\theta}{\partial m}\right)\right.$$
$$+\frac{1}{\cos\gamma}\frac{\partial\gamma}{\partial m}\left(1+r^2\sin\delta\frac{d\theta}{dl}\frac{\partial\theta}{\partial m}\right)+\frac{d\theta}{dl}\frac{\partial}{\partial m}\left(r^2\frac{\partial\theta}{\partial m}\right)-$$
$$\left.\frac{\partial\theta}{\partial m}\frac{d}{dl}\left(r^2\frac{\partial\theta}{\partial m}\right)\right]$$

$$B = \frac{2\omega r}{1+\left(r\frac{\partial\theta}{\partial m}\right)^2}\left[\frac{d\theta}{dl}\sin\gamma - \frac{\partial\theta}{\partial m}\cos(\gamma-\delta)\right]$$

$$C = \frac{2\omega r}{1+\left(r\frac{\partial\theta}{\partial m}\right)^2}\frac{dE_r}{dl}$$

b) The velocity gradient equation in non-blade section is,

$$\frac{\mathrm{d}\upsilon_1}{\mathrm{d}l} = A\upsilon_1 + \frac{C}{\upsilon_1} \tag{3}$$

where,

$$A = \frac{1}{\cos\delta}\left(\frac{\partial\gamma}{\partial m} - \frac{\mathrm{d}\gamma}{\mathrm{d}l}\sin\delta\right) - \frac{\sin\gamma}{r}\sin\delta$$

$$C = -\frac{r^2\omega + r\upsilon_3}{r^2}\frac{\mathrm{d}(r\upsilon_3)}{\mathrm{d}l} + \frac{\mathrm{d}E_r}{\mathrm{d}l}$$

The meaning of variable in the above mentioned equations can be seen from figure 4. Based on two-dimensional flow theory ($\Omega_u = 0$) and iterative calculation of S_1 and S_2 stream surfaces, figure 5 and 6 represent the meridional velocity distribution from hub to shroud along meridional surface streamlines in the whole computational domain of impeller respectively. From the comparison of both, there is a little change of meridional surface velocity distribution in the inlet of domain and there is obvious change of meridional surface velocity distribution in blade area and outlet of impeller.

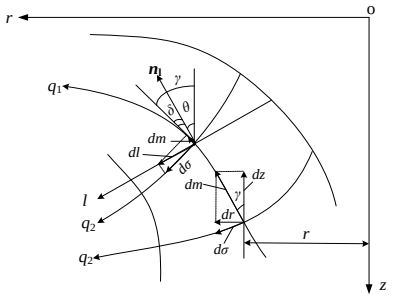

r — radius of meridional surface projection
τ — excretion coefficient
θ — central angle
γ — angle between plumb line and meridional surface streamlines
δ — angle between normal of quasi-orthogonal lines and meridional surface streamlines
ω — rotational angular velocity of impeller
E_r — mechanical energy of relative motion of unit mass fluid

Figure 4. The geometry relationship on S_2 stream surface after introduction of quasi orthogonal line

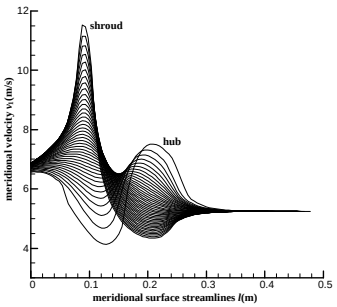

Figure 5. The Meridional velocity distribution based on two-dimensional flow theory($\Omega_u = 0$)

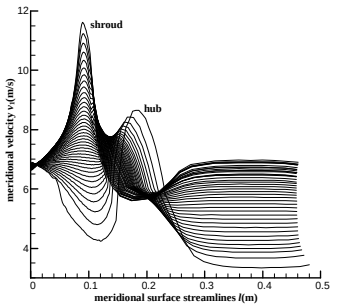

Figure 6. The Meridional velocity distribution obtained by iterative calculation

2.3. Blade camber line confirmation

The circulation differential equation and the blade camber line differential equation are show in equations (4) and (5).

$$\frac{\mathrm{d}(\upsilon_3 r)}{\mathrm{d}q_2} = F(q_1, q_2)\frac{\upsilon_1 r^2}{\upsilon_3 r + \omega r^2} \tag{4}$$

where,

$$F(q_1,q_2)=\left\{\upsilon_1\left[\frac{\partial\gamma}{\partial m}\frac{1}{\cos\delta}-\left(\frac{\partial\gamma}{\mathrm{d}l}\frac{1}{\cos\delta}+\frac{\sin\gamma}{r}+\frac{1}{\tau}\frac{\partial\tau}{\partial m}\right)\sin\delta\right]-\frac{\mathrm{d}\upsilon_1}{\mathrm{d}l}+\frac{1}{\upsilon_1}\frac{\mathrm{d}E_r}{\mathrm{d}l}\right\}\frac{\mathrm{d}l}{\mathrm{d}q_2}$$

There is $dq_2 = 0$ on characteristic line $q_2 = const$.

$$\frac{\mathrm{d}\theta}{\mathrm{d}m} = \frac{\upsilon_3 r + \omega r^2}{\upsilon_1 r^2} \tag{5}$$

Normally, the low pressure edge of blade (the inlet of impeller) and the velocity torque on the low pressure edge of blade are given. The low pressure edge is a characteristic line on meridional surface $\theta = const$. Besides, the velocity torque distribution of hub and shroud is given to draw blade camber lines, the wrapping angle of blade θ can be obtained by equation (5). The quartic polynomial is adopted to show the velocity torque distribution [8] along meridional streamlines when the shape of meridional flow passage as well as the position of inlet and outlet of blade are given. Then, in order to reduce the dependence of experience on designed results, one of the parameters *a* is determined to control the distribution of velocity torque of blade through the theoretical analysis. The simplified quartic distribution function expressed by the follow equation,

$$f(x) = ax^4 + (p-2-2a)x^3 + (3-p+a)x^2 \tag{6}$$

Where, the relative length of meridional streamlines in blade area can be expressed by $x = l / l_0$.

The designed pump chooses *p*=0，*a*=1.6. The velocity torque distribution of hub in blade area is shown in figure 7.

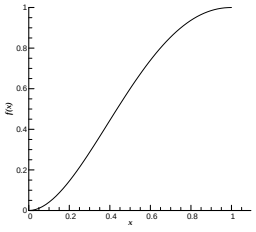

Figure 7. The velocity moment distribution of hub on blade

2.4. Thickening and smoothing of blades

Blades are thickened as well as blade leading edges are smoothed in the conformal mapping surface [9]. The spaced guide vanes adopted the same designed method with impeller. Finally, the inlet and outlet of impeller and spaced guide vanes blade after thickening and smoothing can be obtained, the three dimensional model of impeller and spaced guide vanes can be seen in figure 8.

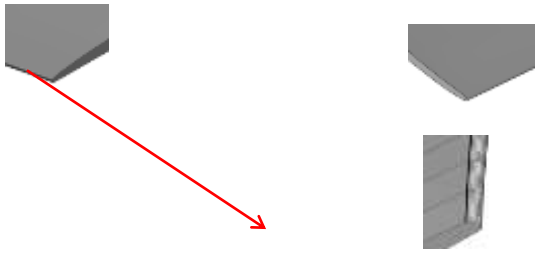

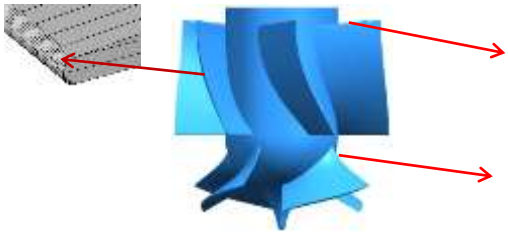

Figure 8. The three dimensional model of impeller and spaced guide vanes

3. Numerical simulation and results analysis

The whole flow passage geometrical model of designed pump is shown in figure 9. In order to compare with the hydraulic performance of 211-80 model pump conveniently, the calculation choose the same eight operating point, the corresponding flow rate are 1728.0, 1671.3, 1551.7, 1499.8, 1457.7, 1347.2, 1224.2 and 1118.8m^3/h.

Unstructured tetrahedral mesh discrete calculation domain is adopted under the comprehensive consideration of time and accuracy. The meshing result is shown in figure 10. Table 1 shows grid independence test results. The influence of grid number on numerical calculation results can be ignored when the correlation of head and efficiency with different grid number is lower than 1%. The finalized total grid number of designed pump is 242 million.

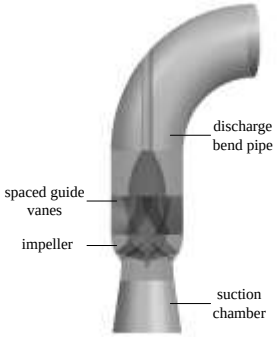

Figure 9. The whole flow passage geometrical model

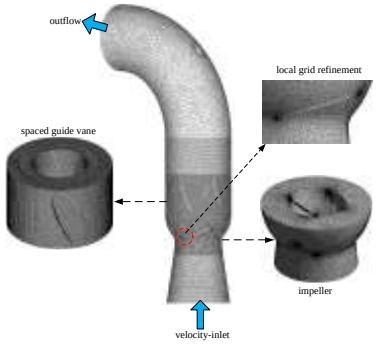

Figure 10. The grid of designed pump

Table 1. The head and efficiency of designed mixed-flow pump with different grids of impeller

numerical order	impeller	entirety	Head H (m)	Efficiency η (%)
1	680487	1707715	5.79	87.47
2	1088790	2116018	5.78	87.36
3	1396984	2424212	5.70	87.73
4	1609834	2637062	5.77	87.38

The RNG turbulent model and SIMPLE algorithm are applied to solve the RANS equations. The Multiple Reference Frame (MRF) model is applied to take into account the interaction between stationary parts and rotating impeller. For such calculations, standard wall functions based on the logarithmic law have been used. Standard Scheme has been used for pressure terms and second-order upwind discretization scheme has been used for convection terms. The boundary conditions are as follows: inlet is the velocity inlet and assumed as a uniform distribution, outflow is given as boundary condition at outlet, and the solid walls with non-slip condition such as blade surface, hub and shroud are given the moving wall.

3.1. The performance curves

The flow rate–head curve and flow rate-efficiency curve of designed pump and model pump can be seen from figure 11. From the figure 11, it can be seen that, the experimental results and CFD simulation results is basically consistent. Thus the reliability of the numerical model was validated. In figure 11, the imaginary line A represents low flow rate condition ($0.78Q_d$), the imaginary line B represents optimal flow rate condition, the imaginary line C represents high flow rate condition ($1.16Q_d$). Compared with the simulation results of model pump, the head of designed pump increases 0.81m and the hydraulic efficiency of designed pump increases 9.1% at B flow rate condition. The hydraulic efficiency of designed pump increases 6.46% at A flow rate condition. In general, the designed pump can restrain the phenomenon of a sudden drop of hydraulic efficiency and the high efficiency areas of designed pump broaden significantly in high flow rate conditions.

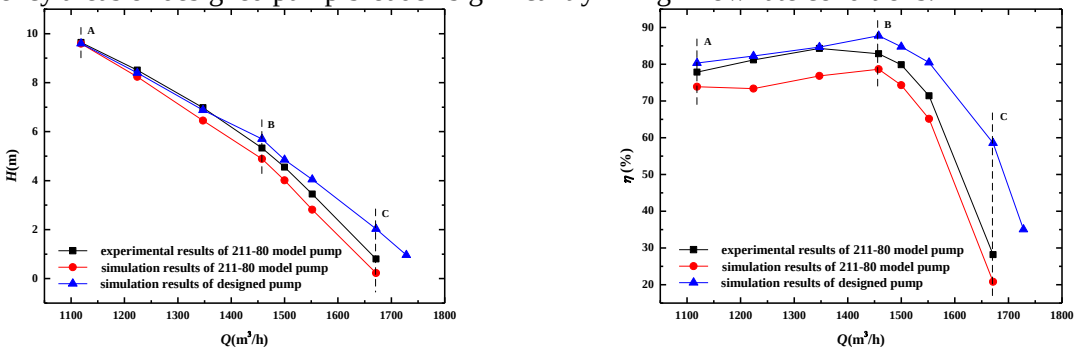

a) Flow rate-head curve b) Flow rate- efficiency curve

Figure 11. The comparison of performance curves between designed pump and 211-80 model

3.2. The analysis of inner flow field

The static pressure distribution is as shown in figure 12. From the distribution of static distribution can be seen that, with the increase of flow rate, static pressure decreases at same location of impeller. The static pressure distributions are relatively uniform. There is no obvious flow separation phenomenon.

$Q=1118.8$ (㎥/㎰) $Q=1457.7$ (㎥/㎰) $Q=1671.3$ (㎥/㎰)

Figure 12. The static pressure distribution of designed impeller under different flow conditions

Figure 13 shows the velocity distribution (unit m/s) of impeller and local amplification of velocity distribution on blade inlet under different flow rate conditions. From the figure 13, it can be seen that, there is no obvious impact phenomenon that at inlet of impeller blade. At low flow rate condition ($Q=1118.8$ (m^3/h)), the directions of velocity at blade inlet change obviously, the distribution of velocity is uninform. With the increase of flow rate, the distributions of velocity become more and more uniform, it is benefit to improve the hydraulic performance. And the velocity increases at same location of impeller blade with the increase of flow rate, the velocity distribution is still uniform, there is no obvious phenomenon of flow separation.

$Q=1118.8$ **(m^3/h)** $Q=1457.7$ **(m^3/h)**

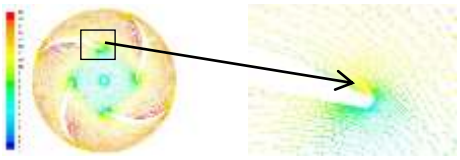

$Q = 1671.3$ **(m³/h)**

Figure 13. The velocity distribution (unit m/s) of impeller and local amplification of velocity distribution on blade inlet under different flow rate conditions

In order to observe the streamlines distribution of designed pump, figure 14 show the streamlines distribution of inner flow field of midsection which is parallel to axis of designed pump. From the figure 14, it can be seen that the streamlines distribution is uniform at three different flow rate conditions, and there is no backflow phenomenon caused by flow separation at outlet of pump. There is also no obvious wake shedding vortex phenomenon from impeller outlet to guide vane inlet.

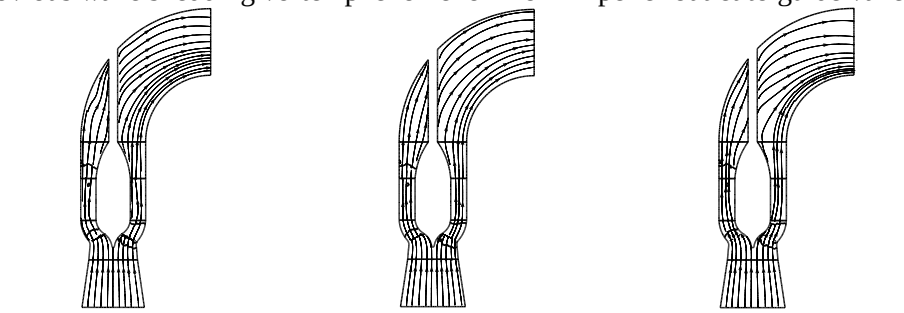

$Q = 1118.8$ $Q = 1457.7$ $Q = 1671.3$

Figure 14. The Streamlines distribution of inner flow field

4. Conclusion

(1) This paper completed the quasi-three dimensional hydraulic design of impeller and spaced guide vanes of high specific speed mixed-flow pump which specific speed is 819. The meridional speed distribution got by the iterative calculation of S_1 and S_2 stream surfaces is obviously different from the meridional speed distribution got by the traditional two dimensional theory($\Omega_u = 0$), and the former is close to the actual flow.

(2) Compared with the 211-80 model, the high specific speed mixed-flow pump designed by the quasi-three dimensional theory has better Hydraulic performance. The hydraulic efficiency of the designed pump on the optimal flow rate condition increases 9.1%. The hydraulic efficiency of designed pump in low flow rate condition (78% designed flow rate) increases 6.46%. The hydraulic efficiency in high flow rate condition areas increases obviously and there is no bad phenomenon of suddenly decrease of hydraulic efficiency in model pump.

(3) The pressure distribution of impeller of designed pump is uniform. There is no obvious impact phenomenon on impeller inlet. The stream lines distribution of whole designed pump is gentle, and there is no obvious wake shedding vortex phenomenon from impeller outlet to guide vane inlet.

Reference

[1] Zhang X T, Ji C J, Gao G H, et al. 2012 Study on hydraulic design method of mixed-flow pump impeller [J]. *Pump technology*, **1**: 23-27.
[2] Bing H, Zhang Q Z, Cao S L, et al. 2013 Iteration design of direct and inverse problems and flow analysis of mixed-flow pump impellers [J]. *J Tsinghua Univ (Sci&Tech)*, **53(2)**:179-183.
[3] Bing H, Cao S L 2013 Multi-parameter optimization design, numerical simulation and performance test of mixed-flow pump impeller. *Science China Technological Sciences* 56.
[4] Kim S, Lee K Y, Kim J H, et al. 2015 High performance hydraulic design techniques of mixed-flow pump impeller and diffuser [J]. *Journal of Mechanical Science and Technology*, **Vol.29 (1)**:227-240.
[5] Liu Q 2006 Numerical Simulation of Interior Flow for High Specific Speed Mixed-flow Pump and Its Characteristics Prediction [D]. *Jiang Su: Jiang Su University Thermal Engineering department.*
[6] Guan X F 2011 *Modern Pumps Theory and Design* [M]. Beijing: China Astronautic Publishing House, 2011:471-472.
[7] Lin K, Cao S L, Zhu B S, et al. 2008 Flow computations for the design of high specific speed mixed-flow pumps [J]. *J Tsinghua Univ (Sci&Tech)*, **48(2)**:219-223.
[8] Zhang Q Z, Cao S L, Wang H, et al. 2011 Effects of velocity moment distribution law on design of mixed-flow pump impeller [J]. *Journal of Drainage and Irrigation Machinery Engineering*, **29(3)**.
[9] Cao S L, Liang L, Zhu B S, et al. 2005 Design method for impeller of high specific mixed-flow pump [J].*Journal of Jiangsu University(Natural Science Edition)*, **26(3)**.